University of Groningen

Highly abundant HCN in the inner hot envelope of GL 2591

Boonman, A. M. S.; Stark, R.; Tak, F. F. S. van der; Dishoeck, E. F.; Schafer, F.; Lange, G de; Laauwen, W. M.; van der Wal, P.B.

IMPORTANT NOTE: You are advised to consult the publisher's version (publisher's PDF) if you wish to cite from it. Please check the document version below.

Document Version
Publisher's PDF, also known as Version of record

Publication date:
2001

[Link to publication in University of Groningen/UMCG research database](#)

Highly abundant HCN in the inner hot envelope of GL 2591: probing the birth of a hot core?

A.M.S. Boonman

Sterrewacht Leiden, P.O. Box 9513, 2300 RA Leiden, The Netherlands

R. Stark and F.F.S. van der Tak

Max-Planck-Institut für Radioastronomie, Auf dem Hügel 69, D-53121 Bonn, Germany

E.F. van Dishoeck

Sterrewacht Leiden, P.O. Box 9513, 2300 RA Leiden, The Netherlands

P.B. van der Wal and F. Schäfer

Max-Planck-Institut für Radioastronomie, Auf dem Hügel 69, D-53121 Bonn, Germany

and

G. de Lange and W.M. Laauwen

Space Research Organisation of the Netherlands (SRON), P.O. Box 800, 9700 AV Groningen, The Netherlands

ABSTRACT

We present observations of the ν_2=0 and vibrationally excited ν_2=1 J=9–8 rotational lines of HCN at 797 GHz toward the deeply embedded massive young stellar object GL 2591, which provide the missing link between the extended envelope traced by lower-J line emission and the small region of hot ($T_{\mathrm{ex}} \geq 300$ K), abundant HCN seen in 14 μm absorption with the *Infrared Space Observatory (ISO)*. The line ratio yields T_{ex}= 720^{+135}_{-100} K and the line profiles reveal that the hot gas seen with *ISO* is at the velocity of the protostar, arguing against a location in the outflow or in shocks. Radiative transfer calculations using a depth-dependent density and temperature structure show that the data rule out a constant abundance throughout the envelope, but that a model with a jump of the abundance in the inner part by two orders of magnitude matches the observations. Such a jump is consistent with the sharp increase in HCN abundance at temperatures $\gtrsim 230$ K predicted by recent chemical models in which atomic oxygen is driven into water at these temperatures. Together with the evidence for ice evaporation in this source, this result suggests that we may be witnessing the birth of a hot core. Thus, GL 2591 may represent a rare class of objects at an evolutionary stage just preceding the 'hot core' stage of massive star formation.

Subject headings: Circumstellar matter — Line: profiles — ISM: abundances — ISM: molecules — ISM: individual (GL 2591) — Radiative transfer

1. Introduction

Molecules are important tools to investigate the physical and chemical structure of the envelopes around massive young stars. Physical models are a prerequisite for determining molecular abundance profiles, which in turn are powerful evolutionary indicators (van Dishoeck & Blake 1998). HCN is a particularly important molecule because it has pure rotational lines in the submillimeter and ro-vibrational lines in the infrared part of the spectrum, which can both be observed from the ground. The combination of submillimeter emission and infrared absorption gives strong constraints on the structure and geometry of the sources (Carr et al. 1995; van der Tak et al. 1999, 2000). It also provides independent information on the level populations and thus allows a study of the excitation mechanisms present in these objects. HCN is one of the more abundant nitrogen-bearing species in dense clouds and plays a key role in the nitrogen chemistry in hot cores (Viti & Williams 1999; Rodgers & Charnley 2001). Therefore it might also be a good candidate to probe the on-set of the 'hot core' phase in massive star-forming regions. This is the phase just before the ultra compact H II region is formed, in which the massive embedded young star still has a high accretion rate, but begins to ionize its surrounding material, with thermal pressure creating a warm dense neutral shell. The hot core phase is characterized by weak radio continuum emission, evaporation of ices, and high-temperature chemistry ($T \gtrsim 300$ K) leading to enhanced gas-phase molecular abundances with respect to earlier evolutionary phases and the production of complex molecules, such as CH_3OCH_3 and CH_3CN (Kurtz et al. 2000).

HCN has been detected toward many massive star-forming regions in the submillimeter and the infrared (e.g. Ziurys & Turner 1986; Evans, Lacy, & Carr 1991; Carr et al. 1995). Typical HCN abundances toward massive protostars that do not show the presence of a hot core are $\sim 10^{-9}$–10^{-8}, derived from submillimeter observations (Schreyer et al. 1997). Even most hot cores, which are predicted to have enhanced gas-phase HCN abundances, show typical HCN abundances of $\sim 10^{-9}$–10^{-8}, based on low-J submillimeter lines (Hatchell, Millar, & Rodgers 1998). On the other hand, observations with the *Infrared Space Observatory (ISO)* of the ν_2 ro-vibrational band around 14 μm toward a dozen massive young stars thought to precede the 'hot core' phase have revealed strong HCN absorption indicating that hot gas ($T_{ex} > 300$ K) is present with abundances up to 10^{-6} (Lahuis & van Dishoeck 2000). Such high HCN abundances have been derived in very few massive star-forming regions from millimeter data, and, except for Orion, the high estimates are mostly based on interferometric observations of a single low-J isotopic transition, leading to large uncertainties in the derived HCN abundances (Carral & Welch 1992). Most of the well-known hot cores such as W 3(H_2O) and G 34.3, which show a wealth of complex organic molecules, are too weak at mid-infrared wavelengths to observe through infrared absorption with current instrumentation. The high frequency submillimeter data presented here provide an alternative method to probe

abundant HCN.

The low spectral resolution of the *ISO* data ($R = \lambda/\Delta\lambda \sim$1500 at 14 μm) allows no kinematical information to be derived for the hot abundant HCN gas and therefore its origin is not clear, in particular whether it is located in the inner hot part of the envelope or produced in shocks. Most of the sources showing hot HCN gas also possess significant outflows, so that shock chemistry cannot be ruled out. This is especially the case for the massive protostar GL 2591, where a significant outflow component is seen in infrared CO absorption lines (Mitchell et al. 1989; van der Tak et al. 1999). High-resolution heterodyne spectroscopy of high-J rotational lines can distinguish between these two explanations. We present here observations of the HCN ν_2=0 J=9–8 line and the first detection of the vibrationally-excited ν_2=1 J=9–8 line of HCN at 797.330 GHz toward the massive protostar GL 2591. So-far, the highest observed rotational transitions of HCN in this source are the ν_2=0 J=4–3 and the vibrationally excited ν_2=1 J=4–3 line (van der Tak et al. 1999). The advantage of the J=9–8 transitions is that they have higher excitation energies and can be observed at higher angular resolution than the low-J transitions. In this way, the warmer inner part of the molecular envelope is uniquely probed. Using the low-J HCN, H^{13}CN, and HC^{15}N rotational lines of van der Tak et al. (1999), only an HCN abundance for the outer envelope of GL 2591 could be derived. The addition of the J=9–8 lines allows us for the first time to construct an HCN abundance profile for both the inner and outer envelope. This will help to determine the evolutionary state of this massive protostar, especially whether it has already started the formation of a hot core.

2. Observations

The observations of the HCN ν_2=0 and ν_2=1 J=9–8 lines were made with the MPIfR/SRON 800 GHz heterodyne spectrometer at the James Clerk Maxwell Telescope (JCMT)[1] on 2000 April 19. The spectrometer is based on the MPIfR 795–880 GHz quasioptical SIS-receiver employing standard niobium junction technology with planar tuning circuits fabricated from normal conducting aluminium. The receiver uses an InP Gunn oscillator followed by a doubler and a tripler stage. Details of the setup are described in Schäfer et al. (1997ab). For the measurements described here a prototype waveguide mixer with a diagonal horn was used which consists of a fixed-tuned waveguide mixer with a Nb SIS junction with NbTiN and Al wiring layers. These devices were fabricated at the University of Groningen. Details on the fabrication of similar SIS devices can be found in Jackson et al. (2000). This resulted in a double sideband receiver noise temperature of about 550 K within a band of 50 GHz centered at 810 GHz. The receiver has an intermediate frequency of 3.5 GHz and a bandwidth of 1 GHz. Details of the receiver will be described elsewhere (Stark et al., in preparation). The double sideband observations were taken under dry weather

---

[1]The James Clerk Maxwell Telescope is operated by the Joint Astronomy Centre, on behalf of the Particle Physics and Astronomy Research Council of the United Kingdom, the Netherlands Organization for Scientific Research, and the National Research Council of Canada.

conditions yielding single sideband system temperatures of about 6000 K. The beam size at this frequency is about 8 arcsec full width at half maximum (FWHM) and the main beam efficiency is $\eta_{\mathrm{MB}} \sim 0.2$. The absolute calibration uncertainty is estimated at 50%. The digital autocorrelator spectrometer backend of the JCMT was used with a bandwidth of 500 MHz, yielding a spectral resolution of 378 kHz (~ 0.14 km s^{-1}). The observed spectrum of the massive protostar GL 2591 ($\alpha(1950)=20^h$ 27^m 35.93^s, $\delta(1950)=+40°$ $01'$ $14''.9$), taken by beam switching over $180''$, is shown in Fig. 1 and the integrated line intensities are listed in Table 1.

3.   Results

Two lines are detected in the spectrum of GL 2591 (Fig. 1). The strongest is identified as the J=9–8 rotational transition of HCN in the vibrational ground state ν_2=0. This is the first detection of this line outside Orion (Stutzki et al. 1988). The other line is the first detection of the vibrationally excited ν_2=1 J=9–8 line of HCN at 797.330 GHz in a massive protostar. This line arises from $\sim$1200 K above the vibrational ground state and is therefore an even better probe of the warm gas in this protostar than the ν_2=0 J=9–8 transition which has an excitation energy of $\sim$190 K. Both lines are resolved and can be fit by a single gaussian. The width of the ν_2=0 J=9–8 line is 5.8±0.4 km s^{-1} and of the ν_2=1 line 4.4±0.4 km s^{-1}. The position of the line center of V_{LSR}=–5.1±0.5 km s^{-1} for the ν_2=0 and of V_{LSR}=–6.1±0.5 km s^{-1} for the ν_2=1 line is consistent with the velocity of the quiescent envelope gas of V_{LSR}=–5.5±0.2 km s^{-1} (van der Tak et al. 1999). Although our observation of the CO J=7–6 line in the same beam clearly shows the presence of an outflow component (Fig. 1), the HCN lines have no wings at a level larger than $\sim$17% of the peak intensity, much lower than the $\sim$30% level of the CO J=7–6 wings. This suggests that both HCN J=9–8 lines originate in the warm quiescent gas of the molecular envelope. Moreover, since the vibrationally-excited ν_2=1 J=9–8 and the ground-state ν_2=0 J=9–8 HCN line are observed in the same spectrum and in the same side band, their relative calibration is better than 25%. Also, modeling shows that both lines are optically thin (Table 1), so that their relative strength provides a very accurate handle on the vibrational temperature. We derive T_{ex}=720$^{+135}_{-100}$ K, in excellent agreement with the value T_{ex}=600$^{+75}_{-50}$ K, inferred from the mid-infrared ro-vibrational absorption band observed with *ISO* (Lahuis & van Dishoeck 2000). This strengthens our main argument that the HCN J=9–8 lines and the ro-vibrational absorption band seen with *ISO* probe the same hot region. The continuum present in the spectra is due to warm dust and its level agrees within 30% with the 350 μm continuum photometry of this source (van der Tak et al. 2000).

4.   Models and analysis

The data were analyzed using the temperature and density gradients derived for GL 2591 by van der Tak et al. (2000), shown in Fig. 2. This model is based on submillimeter dust continuum and CS and H$_2$CO line emission data, and also reproduces infrared absorption measurements of

CO. The radiative transfer and excitation of HCN was calculated with the Monte Carlo code of Hogerheijde & van der Tak (2000) on a grid of 40 concentric shells, assuming spherical geometry. The calculations include energy levels up to $J=21$ in both the $\nu_2=0$ and $\nu_2=1$ states, and use collisional rate coefficients by S. Green (see http://www.giss.nasa.gov/data/mcrates). For transitions between vibrational levels, a rate coefficient of 10^{-12} cm^{3}s^{-1} was assumed. Radiative excitation through the 14 μm band due to warm dust mixed with the gas was also included, using grain opacities from Ossenkopf & Henning (1994) and assuming $T_{\rm dust}=T_{\rm gas}$. No external radiation field apart from the 2.73 K cosmic background radiation was applied. Comparison with the observed emission proceeds by convolving the calculated sky brightness with the appropriate beam pattern.

In addition to the HCN $J=9$–8 lines discussed here, the low-J HCN and isotopic lines from van der Tak et al. (1999) (see Table 1) are used for comparison with the model. It was found that this model cannot reproduce the new data using the HCN abundances $x({\rm HCN})= n({\rm HCN})/n({\rm H_2})$ of a few times 10^{-8} indicated by the low-J isotopic lines. This point is illustrated by Model 1 in Table 1. However, using the abundance of $\sim 10^{-6}$ indicated by the $\nu_2=1$ lines and the *ISO* observations overproduces the low-J line data by an order of magnitude. Therefore, a model has been used with different HCN abundances in the inner and outer parts of the circumstellar envelope (Fig. 3). The 'jump' is applied at ≈ 350 AU from the star where $T=230$ K. Chemical models predict that at this gas temperature, reactions of O and OH with H_2 drive atomic oxygen into water (Charnley 1997; Rodgers & Charnley 2001). Interferometric observations of HCN $J=1$–0 already indicated that the HCN enhancement must be limited to a region smaller than 1500 AU where $T > 120$ K and is therefore due to gas-phase reactions rather than ice evaporation at $T \sim 90$ K (van der Tak et al. 1999).

Increasing the HCN abundance in the inner envelope by a factor of 10 (Model 2) still underproduces the observed integrated intensities (Table 1). An HCN abundance of $x({\rm HCN})=10^{-6}$ in the inner envelope, combined with the outer envelope abundance of $x({\rm HCN})=10^{-8}$ (Model 3) reproduces the observed values of the HCN lines within $\sim 10\%$ (Table 1). The inner envelope HCN abundance $x({\rm HCN})=10^{-6}$ corresponds well with the value $x({\rm HCN})=(6.6\pm1.0)\times10^{-7}$ derived for the hot gas from *ISO* observations. The HCN column density derived from the latter model (Table 1) also matches best the value of $N({\rm HCN})=(4\pm0.6)\times10^{16}$ cm^{-2} derived from the same observations by Lahuis & van Dishoeck (2000) and the value for the warm ($T \geq 200$ K) gas of $N({\rm HCN})\sim(3$–$4)\times10^{16}$ cm^{-2} derived from ground-based observations by Carr et al. (1995). The H^{13}CN and HC^{15}N lines are reproduced within a factor of about 2.

Decreasing the inner radius of the model (Fig. 2) by a factor of 3 and extrapolating the temperature and density profile yields similar (within 10%) results for Model 3. The corresponding HCN column density of $N({\rm HCN})=6.6\times10^{16}$ cm^{-2} is somewhat larger than that found from the infrared observations.

Our analysis shows that both $\nu_2=1$ lines and the $\nu_2=0$ $J=9$–8 line are very sensitive to different abundances in the inner envelope, contrary to the $\nu_2=0$ $J=4$–3 line which is optically thick (Table

1) and traces only the outer envelope. The low-J isotopic lines are also sensitive to different abundances in the inner envelope, suggesting that the warm gas contributes significantly to their observed line profiles. This is consistent with the maximum optical depths of ≤ 0.33 derived for these lines (Table 1).

5. Discussion

The HCN abundance of $\sim 10^{-6}$ found here for the inner ($\lesssim 350$ AU) hot envelope of GL 2591 is much higher than predicted by gas-phase models of cold dense clouds of $\sim 10^{-9}$–10^{-8} (Lee, Bettens, & Herbst 1996; Millar, Farquhar, & Willacy 1997; Herbst, Terzieva, & Talbi 2000). Models for high-temperature regions predict, however, HCN abundances of up to $\sim 10^{-6}$–10^{-5} (Caselli, Hasegawa, & Herbst 1993; Charnley 1997; Viti & Williams 1999; Rodgers & Charnley 2001). While the present data do not allow a precise determination of where the jump occurs, our finding is consistent with the recent chemical models by Charnley (1997) and Rodgers & Charnley (2001), who show that above a critical temperature of $230 - 300$ K, the reactions O + H$_2$ $\rightarrow$ OH + H; OH + H$_2$ $\rightarrow$ H$_2$O + H drive most of the atomic oxygen into H$_2$O. This results in low gas-phase O$_2$ and enhanced atomic C abundances, since gas-phase O$_2$ is one of the principal destroyers of atomic C. The formation of atomic C is through cosmic-ray induced photodissociation of CO and thus is not changed. The formation of N$_2$ through NO + N $\rightarrow$ N$_2$ + O is also suppressed at high temperatures, since less NO is available. This provides more reactive atomic nitrogen in the gas-phase. These enhanced atomic C and N abundances result in a significantly increased gas-phase HCN abundance at temperatures $\gtrsim 230$–300 K. Indeed, a recent chemical model by S. Doty (2001, private communication) using the temperature and density gradient of GL 2591 predicts such a sharply increasing HCN abundance profile. The prediction by these models of a large fraction of oxygen in atomic form in the outer envelope and in water in the inner part is consistent with the non-detection of molecular oxygen by the Submillimeter Wave Astronomy Satellite in this region (E. Bergin 2000, private communication). HCN ice has not been detected yet and, as discussed above, interferometric observations indicate that the HCN enhancement cannot be explained by ice evaporation alone. However, ice evaporation of other species such as H$_2$O, CO$_2$, and C$_2$H$_2$ has occurred for GL 2591 (van Dishoeck 1998). Together with the evidence for high-temperature chemistry inferred for HCN, this suggests that we may be witnessing the formation of a hot core in GL 2591. Thus, GL 2591 may represent a rare class of objects at an evolutionary stage just preceding the 'hot core' stage of massive star formation.

Inclusion of a chemistry network in the modeling will allow a refinement of our abundance profile. Interferometric observations of high-J HCN transitions at sub-arcsecond resolution are needed to determine the temperature at which the jump takes place more accurately. So-far, such a high HCN abundance as derived for the inner part of the molecular envelope in GL 2591 has been observed in very few massive star-forming regions other than Orion. Therefore observations of high-J HCN vibrational ground-state and vibrationally-excited ν_2=1 rotational lines toward other

massive protostars, including hot cores, will allow a comparison of abundance profiles between these sources and search for evolutionary effects. Finally, high-resolution observations of other 'hot core' molecules, such as CH_3OCH_3 in the submillimeter or C_2H_2 in the infrared, may confirm the presence of a hot core in GL 2591.

REFERENCES

Carr, J. S., Evans, N. J. II, Lacy, J. H., & Zhou, S. 1995, ApJ, 450, 667

Carral, P., & Welch, W. J. 1992, ApJ, 385, 244

Caselli, P., Hasegawa, T. I., & Herbst, E. 1993, ApJ, 408, 548

Charnley, S. B. 1997, ApJ, 481, 396

Evans, N. J. II, Lacy, J. H., & Carr, J. S. 1991, ApJ, 383, 674

Hatchell, J., Millar, T. J., & Rodgers, S. D. 1998, A&A, 332, 695

Herbst, E., Terzieva, R., & Talbi, D. 2000, MNRAS, 311, 869

Hogerheijde, M. R., & van der Tak, F. F. S. 2000, A&A, 362, 697

Jackson, B. D., de Lange, G., Laauwen, W. M., Gao, J. R., Iosad, N. N., & Klapwijk T. M. 2000, Proc. of the 11th Int. Symp. on Space THz Technology, in press

Kurtz, S., Cesaroni, R., Churchwell, E., Hofner, P., & Walmsley, C. M. 2000, in Protostars and Planets IV, ed. V. Mannings, A. P. Boss, & S. S. Russell (Tucson: University of Arizona Press), 299

Lahuis, F., & van Dishoeck, E. F., 2000, A&A, 355, 699

Lee, H.-H., Bettens, R. P. A., & Herbst, E. 1996, A&AS, 119, 111

Millar, T. J., Farquhar, P. R. A., & Willacy, K. 1997, A&AS, 121, 139

Mitchell, G. F., Curry, C., Maillard, J-P., & Allen, M. 1989, ApJ, 341, 1020

Ossenkopf, V., & Henning, Th. 1994, A&A, 291, 943

Rodgers, S. D., & Charnley, S. B. 2001, ApJ, 546, 324

Schäfer, F., van der Wal, P., Kreysa, E., & Gundlach, K. H. 1997a, Proc. of the 8th Int. Symp. on Space THz Technology, ed. R. Blundell & E. Tong (Cambridge: CfA), 566

Schäfer, F., van der Wal, P., Kreysa, E., Lehnert, T., & Gundlach, K. H. 1997b, Proc. of the 5th Int. Workshop on THz Electronics, ed. K. H. Gundlach & M. Carter (Grenoble: IRAM)

Schreyer, K., Helmich, F. P., van Dishoeck, E. F., & Henning, Th. 1997, A&A, 326, 347

Stutzki, J., Genzel, R., Harris, A. I., Herman, J., & Jaffe, D. T. 1988, ApJ, 330, L125

van der Tak, F. F. S., van Dishoeck, E. F., Evans, N. J. II, Bakker, E. J., & Blake, G. A. 1999, ApJ, 522, 991

van der Tak, F. F. S., van Dishoeck, E. F., Evans, N. J. II, & Blake, G. A. 2000, ApJ, 537, 283

van Dishoeck, E. F. 1998, Faraday Discussions, 109, 31

van Dishoeck, E. F., & Blake, G. A. 1998, ARA&A, 36, 317

van Dishoeck, E. F., & van der Tak, F. F. S. 2000, in IAU Symp. 197, Astrochemistry: From Molecular Clouds to Planetary Systems, ed. Y. C. Minh & E. F. van Dishoeck (San Francisco: Astron. Soc. Pac.), 97

Viti, S., & Williams, D. A. 1999, MNRAS, 305, 755

Wilson, T. L., & Rood, R. 1994, ARA&A, 32, 191

Ziurys, L. M., & Turner, B. E. 1986, ApJ, 300, L19

Table 1: Comparison of observed integrated intensities with different model results

Species	Band	Transition	Model 1 K km s^{-1}	Model 2 K km s^{-1}	Model 3 K km s^{-1}	Observed K km s^{-1}	Optical depth[a]
HCN	ν_2=0	J=4–3	19.38	20.09	22.95	24.7[b]	9.9
		J=9–8	14.64	32.52	57.51	60.2	0.14
	ν_2=1	J=4–3	0.11	0.44	2.87	2.5	0.006
		J=9–8	0.39	3.25	22.10	17.1	0.03
H^{13}CN	ν_2=0	J=3–2	1.93	–	3.70	5.5	0.33
		J=4–3	1.05	–	4.72	8.6	0.11
HC^{15}N	ν_2=0	J=3–2	0.45	–	1.03	2.4	0.07
		J=4–3	0.24	–	1.41	3.1	0.03
N(HCN)	$(10^{16}$	cm$^{-2})$	0.12	0.36	2.7		

[a]The optical depth corresponding to Model 3

[b]The narrow component at V_{LSR}=–5.7 km s^{-1} (van der Tak et al. 1999)

Note. — Model 1: Constant abundance x(HCN)=10^{-8}
Model 2: x(HCN)=10^{-8} for T <230 K, x(HCN)=10^{-7} for T >230 K
Model 3: x(HCN)=10^{-8} for T <230 K, x(HCN)=10^{-6} for T >230 K
The model H^{13}CN and HC^{15}N abundances correspond to the HCN abundance divided by the isotopic ratios ^{12}C/^{13}C=60 and ^{14}N/^{15}N=270 respectively (Wilson & Rood 1994)

Note. — Calibration uncertainties in the observed integrated intensities are ∼50% for the J=9–8 lines and ∼30% for the other lines (van der Tak et al. 1999).
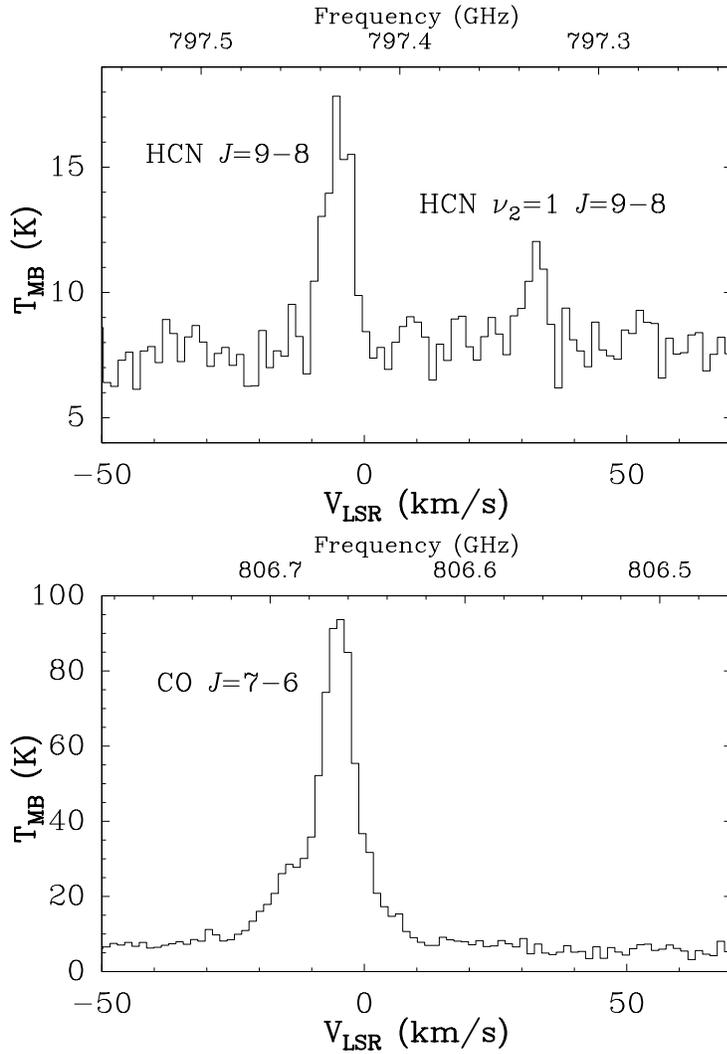
Fig. 1.— Spectrum of the ν_2=0 J=9–8 and the vibrationally excited ν_2=1 J=9–8 line of HCN at 797.434 GHz and 797.330 GHz, respectively, toward the massive protostar GL 2591 (*Top panel*). The spectrum has been smoothed to a spectral resolution of $\sim$1.4 km s^{-1}. The CO J=7–6 line at 806.652 GHz is shown for comparison (*Bottom panel*). The latter spectrum shows clearly the presence of a wing component whereas the HCN J=9–8 lines do not show such a component. The vertical offset shows the submillimeter continuum due to warm dust, which agrees within 30% with the 350 μm continuum photometry of this source (van der Tak et al. 2000).
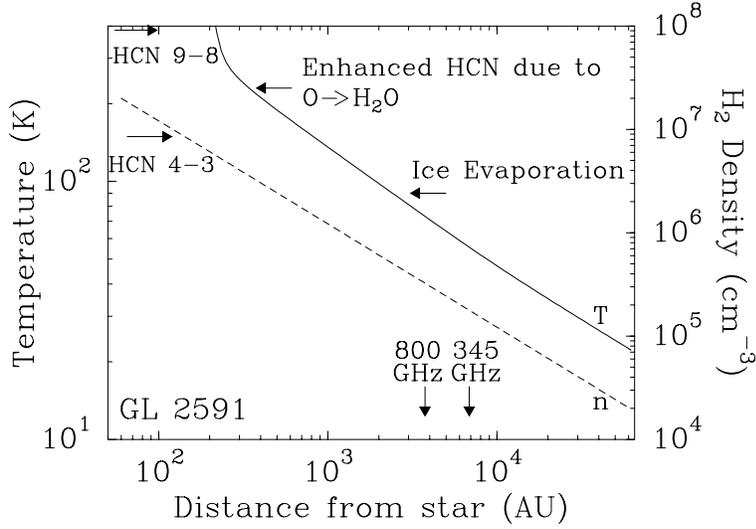
Fig. 2.— Temperature and density structure of GL 2591. The critical densities for the $\nu_2{=}0$ $J{=}9{-}8$ and $\nu_2{=}0$ $J{=}4{-}3$ lines are indicated as well as the JCMT beam sizes at the different frequencies (adapted from van Dishoeck & van der Tak 2000).
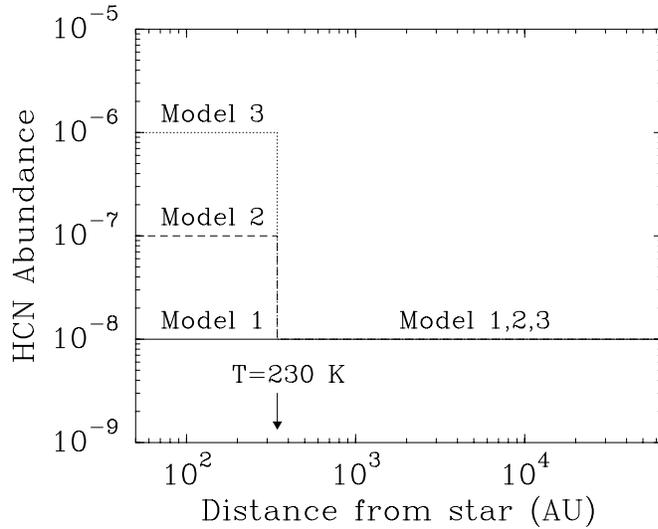

Fig. 3.— Different HCN abundance profiles used in the analysis of §4 (see also Table 1).

H$_2$ Density (cm^{-3})

Temperature (K)

Distance from star (AU)

Enhanced HCN due to

O→H$_2$O

Ice Evaporation

T

n

800 345
GHz GHz

HCN 9–8

HCN 4–3

GL 2591